Modeling of Abdominal Aorta Aneurism Rupture by using Experimental Bubble Inflation Test

Igor Koncar, Dalibor Nikolic, Suzana Pantovic, Mirko Rosic, Nikola Mijailovic, Nikola Ilic, Marko Dragas, Zivan Maksimovic, Lazar Davidovic, and Nenad D. Filipovic, *Member, IEEE*

Abstract— **Aneurysm rupture is a biomechanical phenomenon that occurs when the mechanical stress acting on the inner wall exceeds the failure strength of the diseased aortic tissue. Besides numerous advantages in surgical and anaesthesiological management, emergency procedure leads to fatal outcome in 20-50% of those who reach hospital. Prediction of influence of dynamic blood flow on natural history of aneurysmatic disease and outcome of therapeutic procedures could contribute to treatment strategy and results. In this study we presented experimental design for estimation of the material property of real human aorta tissue from bubble inflation test. Then we investigated fluid-structure interaction of pulsatile blood flow in the specific patient three-dimensional model of abdominal aortic aneurysms (AAAs). Numerical predictions of blood flow patterns and nonlinear wall stresses in AAAs are performed in compliant wall anisotropic model using the finite element method. These computational procedures together with experimental determination of the nonlinear material property could provide us more accurate assessment of aneurysm rupture risk.**

I. INTRODUCTION

Abdominal aorta is susceptible to aneurysm degeneration. Incidence of abdominal aortic aneurysms is increasing and the natural outcome of this degeneration leads to its' rupture and sudden death [1]. Besides numerous advantages in surgical and anaesthesiological management, emergency procedure leads to fatal outcome in 20-50% of those who reach hospital [2,3]. For these reasons preventive surgery, aneurysm repair before rupture occurs, is suggested in patients with AAA is greater than 55mm in diameter. This threshold was established according to Laplace law, since it was believed that diameter is only predictor of rupture. Later, some other independent predictors were found, like chronic obstructive pulmonary disease, tobacco smoking, hypertension, female gender. Still, these factors have not been analyzed sufficiently in order to reach any threshold that includes them and predict rupture. These independent predictors don't have any influence in clinical decision making. For these reason, aneurysm diameter is still the only predictor that suggest decision to expose someone to extensive surgery - elective repair of AAA that has mortality risks of 1-7%.

From everyday practice it was noticed that some small aneurysms with diameter of 55mm or less ruptured or some big aneurysm with diameter greater than 60mm that never ruptured [4,5]. About 8-10% of patients with small aneurysms rupture before overcoming 55mm while around 40% of aneurysms greater that 55mm never rupture [6]. A greatest diameter criterion is based on Laplace law that is related to cylindrical bodies. AAA is rarely cylindrical, and mostly fusiform irregular shape body with numerous curves requiring more detailed analysis of every existing curve. Knowing that, we could assume that in some clinical decision, we are offering surgical treatment too early or too late we should ask if one criterion could fit to all individuals. In order to find answer to that question we need to define the mechanism of rupture and then to explore factors of influence. If rupture is the moment when wall stress overcome the strength of the aortic wall than we need to define these variables in order to find better criteria to predict rupture.

Finite element analysis provides detailed assessment of forces inside the aneurysm wall. Previous works showed correlation between the level of peak wall stress determined with this method and the risk of rupture, and even more, some studies showed that location of the peak wall stress was in correlation with the site of the aneurysm rupture [7,8]. On the other hand, aneurysm wall strength was assessed by different modes, however, these testing were based on uniaxial or biaxial testing [9]

In this study we developed experimental procedure for estimation of the material property of real human tissue arteries from bubble inflation test and computational procedure for simulation of complex fluid-structure interaction of pulsatile blood flow through AAA. The paper is organized as follows. Section II is consisted of description of experimental setup and procedure for bubble inflation test for human aorta tissue and computational methods for simulation of fluid-structure AAA nonlinear by using material properties from experiments. Section III describes some results for computational simulation of pulsatile flow through AAA for a specific patient where shear stress and wall stress distribution were given. Finally some discussion and conclusions remarks are given.

Manuscript received July 31, 2013. This work was supported in part by grants from Serbian Ministry of Education and Science III41007, ON174028 and ON175008.

I. Koncar, N. Ilic, M. Dragas, Z. Maksimovic and L. Davidovic are with Clinic for Vascular and Endovascular Surgery, Serbian Clinical Centre and Medical Faculty, University of Belgrade (e-mail:dr.koncar@gmail.com).

S. Pantovic, M. Rosic are with the Faculty of Medical Science, University of Kragujevac, Serbia (e-mail: spantovic@medf.kg.ac.rs).

N. D. Filipovic, D. Nikolic and N. Mijailovic are with the Faculty of Engineering, University of Kragujevac and BioIRC Kragujevac, Serbia (phone: +381-34-334379; fax: +381-34-333192; e-mail: fica@kg.ac.rs).

978-1-4799-3163-7/13/$31.00 ©2013 IEEE

II. METHODS

A. Experimental setup

Bubble inflation test was used in one study to assess the strength of porcine thoracic aorta, while its' usage in engineering practice is known long time ago. This test simulates natural forces by exposing aortic tissue specimen to inflation with pressurized solution. This was achieved with experimental laboratory model set up. Model consists of the mechanical pump with Crebs-Ringer solution, heater and heat exchanger, tissue container, pressure sensor and transducer with camera. Camera and pressure transducer

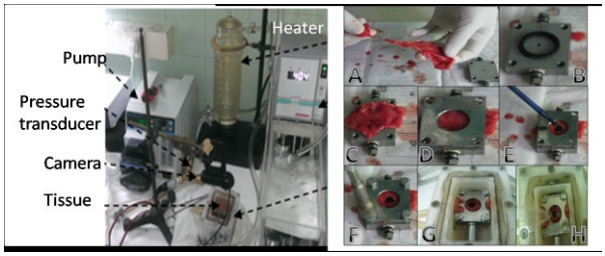

Fig. 1. Experimental setup for bubble inflation test (left). Tissue preparation and testing process (right). A. Tissue tailoring; B. Plate for tissue with a circulated rubber to improve contact; C., D, E, F. Tissue application and coloring; G. Tissue in the container; H. Rupture of the tissue recorded with camera

system are connected by USB connection with the laptop serving as a control unit and data collector. Intraoperative specimen of anterior wall of AAA is harvested during operative treatment of AAA, prepared and placed in the laboratory system. After heating the Crebs-Ringer solution in the system on 37 C, pump is turned on and pressure is gradually increased exposing aortic tissue to the maximum

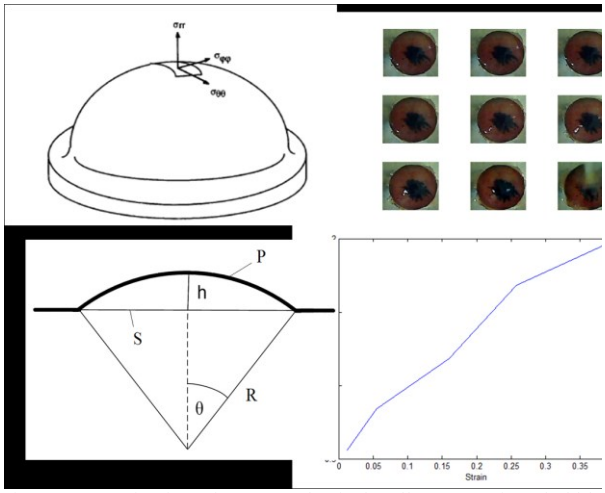

Fig. 2. Determination of aorta mechanical wall property from bubble inflation experiment

pressure of 250 kPa. Tissue was exposed to high pressure until 180s passed, when experiment was interrupted, unless tissue brakes before. Moment of tissue rupture was recorded on a webcam placed above the tissue. Pressure value in the moment of rupture is known due to the software dedicated to follow pressure change and tissue deformation. In order to use data from all analyzed harvested specimens, additional method is developed. All tissue specimens are colored with tissue ink after prepared and placed in the system. Colored circle in the middle of the specimen exposed to the increasing pressure is changing its shape due to tissue deformation. This tissue deformation is than recorded by camera and subsequent images are analyzed according to the changing in the surface area. Ethical board of Serbian Clinical Center approved this research. Defining different subgroups of patients with weaker or stronger wall could improve accuracy of rupture prediction and help physicians in decision making whether to operate or follow patient with abdominal aortic aneurysm. Bubble inflations test provides testing in a most physiological scenario.

B. Fluid computational model

The blood is modeled as the three-dimensional flow of a viscous incompressible fluid described by the Navier-Stokes equations and continuity equation

$$\rho\left(\frac{\partial v_i}{\partial t}+v_j\frac{\partial v_i}{\partial x_j}\right)=-\frac{\partial p}{\partial x_i}+\mu\left(\frac{\partial^2 v_i}{\partial x\partial x_j}+\frac{\partial^2 v_j}{\partial x\partial x_i}\right) \quad (1)$$

$$\frac{\partial v_i}{\partial x_i}=0 \quad (2)$$

where v_i is the blood velocity in direction x_i, ρ is the fluid density, p is pressure, μ is the dynamic viscosity; and summation is assumed on the repeated (dummy) indices, i,j=1,2,3. The first equation represents balance of linear momentum, while the equation (2) expresses incompressibility condition.

Each heart cycle was discretized into 800 uniformly spaced time steps. In the analysis, it was considered that the convergence was reached when the maximum absolute change in the non-dimensional velocity between the respective times in two adjacent cycles was less than 10^{-5}.

The code was validated using the analytical solution for shear stress and velocities through curve tube [10]. A penalty formulation was used in our solver [10].

The incremental-iterative form of the equations for a time step and equilibrium iteration "i" are:

$$\begin{bmatrix}\frac{1}{\Delta t}\mathbf{M}_{\mathbf{v}}+{}^{t+\Delta t}\mathbf{K}_{\mathbf{vv}}^{(i-1)}+{}^{t+\Delta t}\mathbf{K}_{\mu\mathbf{v}}^{(i-1)}+{}^{t+\Delta t}\mathbf{J}_{\mathbf{vv}}^{(i-1)} & \mathbf{K}_{\mathbf{vp}}\\ \mathbf{K}_{\mathbf{vp}}^{\mathbf{T}} & \mathbf{0}\end{bmatrix}\begin{Bmatrix}\Delta\mathbf{v}^{(i)}\\ \Delta\mathbf{p}^{(i)}\end{Bmatrix}=\begin{Bmatrix}{}^{t+\Delta t}\mathbf{F}_{\mathbf{v}}^{(i-1)}\\ {}^{t+\Delta t}\mathbf{F}_{\mathbf{p}}^{(i-1)}\end{Bmatrix} \quad (3)$$

The left upper index "t+Δt" denotes that the quantities are evaluated at the end of time step. The matrix $\mathbf{M}_{\mathbf{v}}$ is mass matrix, $\mathbf{K}_{\mathbf{vv}}$ and $\mathbf{J}_{\mathbf{vv}}$ are convective matrices, $\mathbf{K}_{\mu\mathbf{v}}$ is the viscous matrix, $\mathbf{K}_{\mathbf{vp}}$ is the pressure matrix, and $\mathbf{F}_{\mathbf{v}}$ and $\mathbf{F}_{\mathbf{p}}$ are forcing vectors. The pressure is eliminated at the element level through the static condensation. For the penalty formulation, we define the incompressibility constraint in the following manner:

$$div\mathbf{v} + \frac{p}{\lambda} = 0 \tag{4}$$

where λ is a relatively large positive scalar so that p/λ is a small number (practically zero).

The incremental-iterative form of the equilibrium equations are

$$\left(\frac{1}{\Delta t}\mathbf{M}_{\mathbf{v}} + {}^{t+\Delta t}\mathbf{K}_{\mathbf{vv}}^{(i-1)} + {}^{t+\Delta t}\mathbf{K}_{\mu\mathbf{v}}^{(i-1)} + {}^{t+\Delta t}\hat{\mathbf{K}}_{\mu\mathbf{v}}^{(i-1)} + {}^{t+\Delta t}\mathbf{J}_{\mathbf{vv}}^{(i-1)} + \mathbf{K}_{\lambda\mathbf{v}}\right)\Delta\mathbf{v}^{(i)} = {}^{t+\Delta t}\hat{\mathbf{F}}_{\mathbf{v}}^{(i-1)} \tag{5}$$

where the matrices and vectors are given in [10,11]. Blood flow is simulated for average blood properties: molecular viscosity μ=0.0035 Pa.s and density ρ=1.06 g/cm^3.

C. Material model of the arterial walls

The material model for a three-dimensional arterial wall assumes that the principal directions of the stress tensor coincide with circumferential, axial and radial directions of the artery [12], labeled as the axes 1, 2 and 3, respectively. The strain energy function is given by

$$\psi = \frac{c}{2}\{\exp(Q) - 1\} \tag{6}$$

$$Q = b_1E_1^{\,2} + b_2E_2^{\,2} + b_3E_3^{\,2} + 2b_4E_1E_2 + 2b_5E_3E_2 + 2b_6E_3E_1$$

where c is stress-like material parameter and b_i, $i = 1,...6$ are non-dimensional material parameters.

The non-zero principal Piola-Kirchhoff stress components for a biaxial membrane stress state:

$$S_1 = c\left[(b_1E_1 + b_4E_2 + b_6E_3) - \lambda_3^2\lambda_1^{-2}(b_6E_1 + b_5E_2 + b_3E_3)\right]\exp(Q), \tag{7}$$
$$S_2 = c\left[(b_4E_1 + b_2E_2 + b_5E_3) - \lambda_3^2\lambda_2^{-2}(b_6E_1 + b_5E_2 + b_3E_3)\right]\exp(Q),$$

where the stretch $\lambda_3 = (\lambda_1\lambda_2)^{-1}$ follow from the incompressibility condition $\lambda_1\lambda_2\lambda_3 = 1$.

In the case of constrained biaxial loading when $\lambda_2 = 1$ and $\lambda_1 = \lambda$, we obtain $I_4 - 1 = (\lambda^2 - 1)\cos^2\varphi$, and the stresses are

$$S_1 = c(1-\lambda^{-4}) + 4k_1\cos^4\varphi(\lambda^2-1)\exp[k_2\cos^4\varphi(\lambda^2-1)^2], \tag{8}$$
$$S_2 = c(1-\lambda^{-2}) + k_1\sin^2(2\varphi)(\lambda^2-1)\exp[k_2\cos^4\varphi(\lambda^2-1)^2],$$

while for constrained biaxial loading when $\lambda_1 = 1$ and $\lambda_2 = \lambda$ we have $I_4 - 1 = (\lambda^2 - 1)\sin^2\varphi$, and the stresses become

$$S_1 = c(1-\lambda^{-2}) + k_1\sin^2(2\varphi)(\lambda^2-1)\exp[k_2\sin^4\varphi(\lambda^2-1)^2], \tag{9}$$
$$S_2 = c(1-\lambda^{-4}) + 4k_1\sin^4\varphi(\lambda^2-1)\exp[k_2\sin^4\varphi(\lambda^2-1)^2].$$

D. Fluid-structure interaction algorithm

Fluid-structure interaction problem is considered for AAA blood flow where deformation of aorta walls is included. We used the loose coupling approach for the fluid-structure interaction [12]. The algorithm for this complex problem consists of the following steps:

a) For the current geometry of the blood vessel, determine blood flow with use of the ALE formulation [13]. Wall velocities at the common blood – blood vessel surface are taken as the boundary condition for the fluid.

b) Calculate the loads, arising from the fluid, which act on the walls.

c) Determine deformation of the walls taking the current loads from the fluid.

d) Check for the overall convergence which includes fluid and solid. If convergence is reached, go to the next time step. Otherwise go to step a).

The fluid domain geometry and velocities at the common solid-fluid boundary for the new calculation of the blood flow are updated [14]. For large wall displacements, the FE mesh for the blood flow domain is updated. Go to step a).

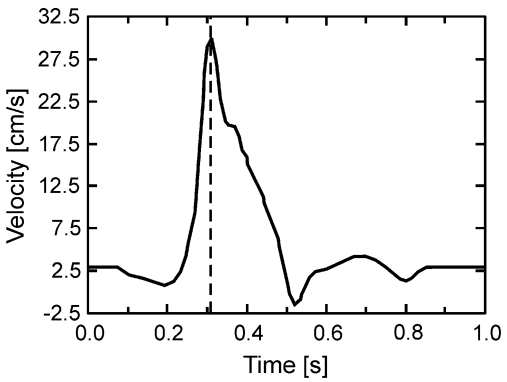

Fig. 3. Input velocity profile. Peak systolic flow occurs at t=0.31 s and diastolic phase begins at t=0.52 s.

III. Results

We calculated time-average Reynolds numbers over the

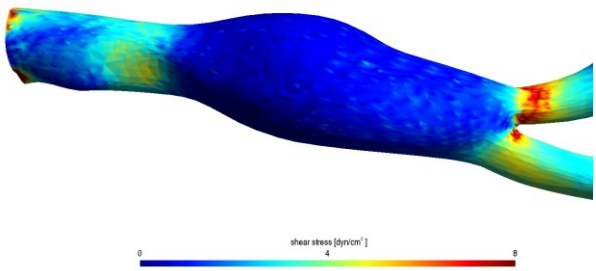

Fig. 4. Wall shear stress distribution for Re_m=300 at t=0.31s

range $50<Re_m<300$, for which the peak Reynolds number is obtained at t=0.31 s and varies over the range $250<Re_{peak}<1500$. The inflow mean velocity is time-dependent and oscillatory, as shown in Fig. 3.

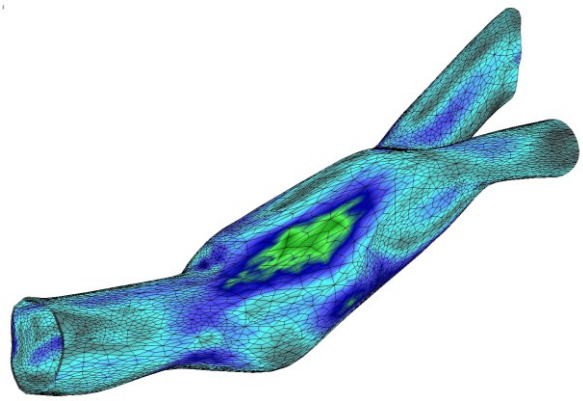

Fig. 5 The von Mises wall stress distribution for Re_m=300 at t=0.29s

A patient specific geometric model of the AAA was created from 1 mm DICOM images of a CT angiography (CTA) study acquired with a multi-detector-row CT scanner. Segmentation was performed using in-house software and the results expressed as a surface triangulation in STL format. Finite element meshes of 8-node 3D element for fluid and solid domains were created with in-house mesh generator. The maximum wall shear stress during the pulsatile cycle was obtained at peak flow, where the velocities and their spatial gradients are greatest (Fig.4). The von Mises wall stress distributions for the aorta wall at t = 0.31 [s] is given in Fig. 5.

It can be observed the behavior of flow patterns and their effect on flow-induced stresses at the AAA material nonlinear wall for physiologically realistic pulsatile blood flow rates.

IV. Discussion and Conclusions

The problem of aneurysms rupture is very important from clinical point of view. The surgical treatment sometime is offering too early or too late if we consider one criterion for all patients. The rupture is the moment when wall stress overcomes the strength of the aortic wall.

We designed the experimental setup for bubble inflation test where we can determine very precise from real aorta patients material properties for wall mechanics. Finite element methods of pulsatile, Newtonian blood flow in three-dimensional compliant nonlinear wall model of abdominal aorta aneurysm have been presented. A three-dimensional anisotropic strain energy functions for wall nonlinear material model is incorporated for fluid-structure interaction model of wall-compliant asymmetric computational model in which both hemodynamics and wall mechanics are computed. These estimations together with experimental determination of the nonlinear material property could provide us more accurate assessment of aneurysm rupture risk. Therefore, the results presented in this paper serve as preliminary predictions for three dimensional patient specific wall-compliant modeling of aneurysms using experimental bubble inflation test.

References

[1] G. O. Young, "Synthetic structure of industrial plastics (Book style with paper title and editor)," in *Plastics*, 2nd ed. vol. 3, J. Peters, Ed. New York: McGraw-Hill, 1964, pp. 15–64.

[2] K.W. Johnston, R.B. Rutherford, M.D. Tilson, et al. "Suggested standards for reporting on arterial aneurysms," *J Vasc Surg* 1991, 13, pp. 452.

[3] K. Ouriel, K. Geary, R.M. Green, et al. "Factors determining survival after ruptured aortic aneurysm: the hospital, the surgeon, and the patient," *J Vasc Surg* 1990, 11(4), pp. 493-496.

[4] L. B. Davidovic, M. D. Markovic, N. S. Jakovljevic, D. Cvetkovic, I. B. Kuzmanovic, D.M. Markovic. „Unusual forms of ruptured abdominal aortic aneurysms," *Vascular* 2008, 16 (1), pp. 17-24

[5] S.A. Choksey, A.B. Wilmink, C.R. Quick, "Ruptured abdominal aortic aneurysm in the Huntingdon district; A 10 year experinece," *Annals of the Royal College of Surgeons of England*, 1999,81, pp. 27-31.

[6] A.J. Hall, E.F.G. Busse, D.J. Mcgarville, J.J. Burgess, "Aortic wall tension as a predictive factor for abdominal aortic aneurysm rupture : Improving the selection of patients for abdominal aortic aneurysm repair," *Ann Vasc Surg* 2000,14, pp. 152-157.

[7] M.F. Fillinger, S.P. Marra, M.L. Raghavan, F.E. Kennedy, "Prediction of rupture risk in abdominal aortic aneurysm during observation: wall stress versus diameter," *J Vasc Surg*. 2003,37, pp. 724-732.

[8] J.D. Barry, A. J. Cloonan, M.T. Walsh, D.A. Vorp, T.M. McGloughlin, "Identification of rupture locations in patient-specific abdominal aortic aneurysms using experimental and computational techniques," *Journal of Biomechanics* 43,2010,pp. 1408–1416.

[9] E.S. Di Martino, A. Bohra, J.P. VandeGest, N.Y. Gupta, M.S. Makaroun, D.A. Vorp, "Biomechanical properties of rupture vs electively repaired abdominal aortic aneurysm wall tissue," *J Vasc Surg* 2006, 43, pp. 570-576.

[10] N. Filipovic, M. Kojic, M. Ivanovic, B. Stojanovic, L. Otasevic, & V. Rankovic, MedCFD, *CFD software for simulation of blood flow through arteries*, University of Kragujevac, 34000 Kragujevac, Serbia, 2008.

[11] N. Filipovic, S. Mijailovic, A. Tsuda, & M. Kojic, "An Implicit Algorithm Within The Arbitrary Lagrangian-Eulerian Formulation for Solving Incompressible Fluid Flow With Large Boundary Motions", *Comp. Meth. Appl. Mech. Eng.*, Vol. 195, No. 44-47, pp. 6347-6361, 2006.

[12] G.A. Holzapfel, C.T. Gasser and R.W. Ogden "A new constitutive framework for arterial wall mechanics and comparative study of material models", *Journal of Elasticity* 61(1-3): 1-48, 2000.

[13] N. Filipovic, M. Kojic and M. Zivkovic, "Viscous Flow in a Collapsible Tube Solved as a Fluid-Structure Interaction Problem", *IASS-IACM*, *Fourth International Colloquium on Computation of Shell & Spatial Structures*, Chania-Crete, Greece, June 5-7, pp 10-24, 2000.

[14] M. Kojic, N. Filipovic, B. Stojanovic, & N. Kojic, *Computer Modeling in Bioengineering – Theoretical Background, Examples and Software*. John Wiley and Sons, 978-0-470-06035-3, England, 2008.